Immunology and Cell Biology (2012), 1–10

www.nature.com/icb

REVIEW

Use of imaging to study leukocyte trafficking in the central nervous system

Elena Zenaro, Barbara Rossi, Stefano Angiari and Gabriela Constantin

The migration of leukocytes from the bloodstream into the central nervous system (CNS) is a key event in the pathogenesis of inflammatory neurological diseases and typically involves the movement of cells through the endothelium of post-capillary venules, which contains intercellular tight junctions. Leukocyte trafficking has predominantly been studied in animal models of multiple sclerosis, stroke and infection. However, recent evidence suggests that immune cells and inflammation mechanisms play an unexpected role in other neurological diseases, such as epilepsy and Parkinson's disease. Imaging leukocyte trafficking in the CNS can be achieved by epifluorescence intravital microscopy (IVM) and multiphoton microscopy. Epifluorescence IVM is ideal for the investigation of leukocyte–endothelial interactions, particularly tethering and rolling, signal transduction pathways controlling integrin activation, slow rolling, arrest and adhesion strengthening in CNS vessels. Multiphoton microscopy is more suitable for the investigation of intraluminal crawling, transmigration and motility inside CNS parenchyma. The mechanisms of leukocyte trafficking in the CNS are not well understood but the use of *in vivo* imaging techniques to unravel the underlying regulatory pathways will provide insight into the mechanisms of brain damage and may contribute to the development of novel therapeutic strategies. In this review, we discuss recent work in this field, highlighting the development and use of *in vivo* imaging to investigate leukocyte recruitment in the CNS.
Immunology and Cell Biology (2012) **0,** 000–000. doi:10.1038/icb.2012.81

Keywords: leukocyte trafficking; intravital imaging; epifluorescence microscopy; multiphoton microscopy; mouse surgical preparation; central nervous system

Leukocyte trafficking in the central nervous system (CNS) plays a key role in neurological diseases involving acute and chronic inflammation. Leukocyte trafficking from the bloodstream into the CNS typically occurs at post-capillary venules, and the barrier function of the CNS endothelium reflects the presence of microvascular endothelial cells with intercellular tight junctions, associated with the interconnected inner and outer endothelial basement membranes.[1,2] End feet projected predominantly by astrocytes form the glia limitans, which is associated with a glial basement membrane. The endothelial and glial basement membranes delimit the perivascular space (Virchow-Robin space).[3]

In order to migrate from the bloodstream into the CNS via parenchymal venules, leukocytes must therefore pass through the endothelial basement membranes into the perivascular space and then through the glia limitans with its distinct basement membrane and astrocytic end feet.[3] However, pial vessels provide an easier route into the CNS for inflammatory cells because they lack the glia limitans and perivascular space, and their tight junctions have a different composition to parenchymal vessels.[1,4] Leukocytes may also migrate into the CNS by crossing the endothelium of choroid plexus vessels (which lack tight junctions) but in this case they also need to pass through an epithelial layer with tight junctions in order to reach the cerebrospinal fluid (CSF).[3,5]

The mechanisms of leukocyte trafficking in the CNS have been studied in experimental models relevant to multiple sclerosis (MS), and its animal model experimental autoimmune encephalomyelitis (EAE). MS and EAE are autoimmune diseases characterized by perivascular inflammatory infiltrates, mainly comprising lymphocytes and monocytes.[6] Inflammatory cells entering the CNS to induce EAE must first migrate into the subarachnoid space (SAS) by crossing the blood–CSF barrier in choroid plexus vessels, or by migrating through pial vessel walls.[3] T cells are reactivated in the SAS at the contact with antigens, which is required for subsequent migration through CNS parenchymal vessels.[7]

Immune cell recruitment in the CNS has also been studied in ischemic stroke models. The brain endothelium releases cytokines and chemokines shortly after the onset of stroke, leading to the recruitment of neutrophils, monocytes and lymphocytes, which secrete inflammatory mediators, activate microglia and induce neuronal damage.[8,9] In addition, studies on the mechanisms of leukocyte trafficking have been performed in animals infected with Plasmodium bergei, a common disease model of cerebral malaria.[10–12] Although the adhesion molecules mediating leukocyte–endothelial interactions are still unclear, blockade of CXCL10-dependent leukocyte trafficking consistently reduces mortality of Plasmodium berghei-infected mice.[12]

Department of Pathology and Diagnostics, University of Verona, Verona, Italy
Correspondence: Dr G Constantin, Department of Pathology and Diagnostics, Section of General Pathology, University of Verona, Strada le Grazie 8, Verona 37134, Italy.
E-mail: gabriela.constantin@univr.it
Received 15 November 2012; revised 26 November 2012; accepted 27 November 2012

We have recently shown that seizures induce the expression of vascular cell adhesion molecules allowing leukocyte rolling and arrest in cortical vessels, mediated by the leukocyte mucin PSGL-1 (P-selectin glycoprotein ligand) and integrins VLA-4 and LFA-1.[13] The inhibition of leukocyte–vascular interactions either by blocking them with antibodies, or in mice genetically deficient in functional adhesion molecules, has been shown to substantially reduce seizures. In support of these data, recent studies in a model of viral meningitis showed that myelomonocytic cell recruitment induces vascular leakage resulting in lethal seizures.[14] Furthermore, there is increasing evidence that chronic inflammation, loss of blood–brain barrier (BBB) integrity and immune cell migration play a significant role in Parkinson's disease,[15,16] suggesting that leukocyte trafficking in the CNS is an underappreciated pathophysiological process in other neurological diseases.

Leukocyte recruitment from the circulation involves a tightly regulated sequence of steps controlled by adhesion molecules and activating factors.[17,18] The adhesion cascade in inflamed post-capillary venules is often described in terms of four 'classical' steps:[19] (1) capture (tethering) and rolling, mediated by interactions between selectins and mucins, and between integrins and members of the immunoglobulin (Ig) superfamily; (2) activation, during which signaling through the $G\alpha_i$ pathway is induced by chemoattractants and leads to the activation of integrins; (3) arrest, which is mediated by leukocyte integrins and their endothelial counter-ligands; and (4) diapedesis/transmigration. More recently, several additional steps have been defined, including slow rolling, adhesion strengthening and spreading, intravascular crawling, and transcellular and paracellular transmigration.[19]

A major bottleneck in the characterization of mechanisms controlling leukocyte recruitment in the CNS is the direct visualization and analysis of leukocyte–endothelial interactions in the microcirculation or inside the parenchyma of living animals. Several groups have recently overcome this limitation by using intravital microscopy (IVM) to uncover some of the mechanisms controlling the adhesion cascade in CNS venules. Epifluorescence IVM was applied in the brain and spinal cord pial venules and helped to identify the role of selectins and integrins in primary and secondary leukocyte adhesion. This provided important qualitative and quantitative data concerning the molecular mechanisms that control leukocyte–endothelial interactions in inflamed CNS venules in animal models relevant to MS/EAE, stroke and epilepsy, and provided insights into the adhesive capabilities of different leukocyte subpopulations.[13,20–26] However, although epifluorescence IVM allows the optimal visualization of pial vessels, its ability to image parenchymal venules remains severely limited.

More recently, two-photon laser scanning microscopy (TPLSM) in the CNS has allowed the deeper parenchymal imaging of neural structures and immune cell trafficking. This minimally invasive approach has revolutionized the study of the nervous system[27] and has been used to study the development and plasticity of synaptic connections,[28] neuronal network activity,[29] cerebral vasculature[30] and amyloid plaques.[31] TPLSM has also been used to study leukocyte recruitment in the spinal cord in EAE models[32,33] and in the brain following viral infections,[14,34] but the analysis of leukocyte trafficking in the CNS using this method is still in its infancy. In this review, we summarize recent advances in CNS imaging using epifluorescence IVM for the analysis of leukocyte–endothelial interactions and describe the fundamental steps required to achieve successful IVM imaging in the brain and spinal cord. We also consider novel aspects of leukocyte imaging in parenchymal vessels and inside the neuropil using TPLSM in the mouse cortex and spinal cord, and finally we discuss future perspectives in CNS imaging.

EPIFLUORESCENCE IVM IN THE CNS

The CNS is considered an immunologically privileged site and few leukocytes are present under normal circumstances.[35] The expression of adhesion molecules on the CNS vasculature, both under normal conditions and when inflammation is triggered, is also significantly lower than in other tissues.[20] The inflamed brain endothelium can mediate the adhesion of lymphocytes but the non-inflamed endothelium cannot.[22] The systemic delivery of pro-inflammatory molecules such as LPS (lipopolysaccharide) and TNFα (tumor necrosis factor α) induces the expression of E-selectin, P-selectin and integrin ligands such as VCAM-1 (vascular cell adhesion molecule) and ICAM-1 (intercellular adhesion molecule) to promote leukocyte adhesion.[3,20,22] These adhesion molecules also mediate interactions between inflammatory cells and the CNS endothelium in animal models of EAE, stroke and epilepsy.[3] During such inflammatory reactions, adhered leukocytes can induce direct endothelial damage, increasing the permeability of the BBB and favoring leukocyte trafficking from the bloodstream into the CNS parenchyma.[36,37] Despite the recent development of more sophisticated techniques, epifluorescence IVM remains the principal method to study leukocyte–endothelial interactions in CNS vessels. This approach facilitates the analysis of: (1) adhesion molecules and their role in leukocyte capture (tethering) and rolling; (2) the role of $G\alpha i$ proteins and chemoattractant-triggered signal transduction pathways controlling integrin activation; (3) adhesion molecules and their role in leukocyte arrest; (4) the mechanisms of slow rolling; and (5) the mechanisms controlling adhesion strengthening.

EPIFLUORESCENCE IVM IN BRAIN PIAL VESSELS

Epifluorescence IVM has been used to image brain pial vessels in mice treated with pro-inflammatory agents or in mice with EAE. We showed that the expression of adhesion molecules such as E-selectin, P-selectin, VCAM-1 and ICAM-1 in mice with preclinical EAE was mimicked by the systemic injection of TNFα or LPS.[22] We found that the PSGL-1 and integrin α_4 were crucial for activated T-cell rolling in the inflamed brain venules,[22,25] whereas integrins α_4 and lymphocyte function-associated antigen (LFA-1) were required for T-cell arrest.[22] In agreement with our data, Kerfoot *et al.*[24,26] found that leukocytes interacted with the inflamed brain pial endothelium during preclinical EAE, in a manner dependent on P-selectin and integrin α_4.

We have recently shown that seizures induce the expression of vascular cell adhesion molecules in brain venules allowing leukocyte rolling and arrest in cortical vessels, mediated by PSGL-1 and leukocyte integrins VLA-4 and LFA-1.[13] The loss of BBB integrity, which is known to enhance neuronal excitability, was induced by acute seizures, but was prevented by blocking leukocyte–vascular adhesion, suggesting a pathogenic link between leukocyte–vascular interactions, BBB damage and seizures. Our data were supported by recent studies in a model of viral meningitis showing that myelomonocytic cell recruitment causes vascular leakage and acute seizures.[14] Furthermore, we and others have validated the results produced in animal seizure models by demonstrating the accumulation of perivascular leukocytes in the brains of epilepsy patients.[13,38]

Epifluorescence IVM in brain pial vessels has been also performed in Plasmodium berghei-infected mice.[10–12] These studies have shown that P-selectin and ICAM-1 are necessary for platelet, but not leukocyte, rolling and arrest,[10,11] and demonstrated that CXCL10

chemokine is important for leukocytes adhesion in brain venules and subsequent migration in the parenchyma.[12]

The analysis of leukocyte–endothelial interactions in brain venules by epifluorescence IVM is usually carried out through a cranial window, which requires the artificial ventilation of test animals and carries associated risks of bleeding and tissue overheating from cautery. This is necessary because blood leukocytes are typically labeled with Rhodamine 6G, which cannot be visualized efficiently through the skull. We have established an epifluorescence IVM technique allowing the visualization of superficial cerebral vessels through the largely transparent intact parietal skull in young mice. This approach is suitable for cortical pial vessels but can visualize to some extent parenchymal vessels (50–100 μm in depth), which are penetrating branches of pial vessels responsible for cortex vascularization.[13,22,39] Animals are deeply anesthetized and maintained at 37 °C using a stage-mounted strip heater. A heparinized PE-10 polyethylene catheter is inserted into the right common carotid artery towards the brain for the injection of fluorescent leukocytes (Figure 1a). In order to exclude non-cerebral vessels (bone, bone marrow and meningeal vessels), the right external carotid and pterygopalatine arteries are ligated.[22] The pterygopalatine artery is an extracranial branch of the internal carotid, which predominantly vascularizes extracranial structures. This gives rise to the middle meningeal artery, a branch that must be excluded because IVM is used to visualize beneath these vessels in the parietal cortex. The mouse is placed under the epifluorescence microscope on a large and motile stage equipped with water immersion objectives (Figure 1b). The images are then visualized using a high-performance video camera suitable for low-level fluorescence.[22] Arterioles are easily identified as vessels with divergent bifurcations, whereas confluent branches define venular segments.[40] Blood vessels can be visualized through the skull using high-molecular-weight fluorescent dextran, which is injected slowly into a heparinized catheter connected to a digital pump before cell injection. Many branches of the pial cerebral venules have a characteristic 'interrupted' shape with convex origins, reflecting their emergence on the brain surface from deeper cortical layers (Figure 1c). This peculiarity of cerebral veins makes them easily recognizable and clearly distinguishes them from bone vessels (thin and *Y*-shaped) and meningeal vessels (thin and elongated, with few branches), which are also in a different focal plane to the pial vessels. Bone marrow vessels are found at bone sutures in a more superficial focal plane, creating a rich honeycomb net at the coronal suture.[41] The wall shear stress (WSS) in brain venules is higher than other organs but it is always 2–3 times lower than in arterioles.[42] No adhesive interactions are normally observed in the brain arterioles (Figure 1d).

EPIFLUORESCENCE IVM IN SPINAL CORD VENULES

Leukocyte trafficking in EAE occurs preferentially in the white matter of the spinal cord. Early studies suggested that inflammatory cells arrive initially in the SAS during preclinical EAE.[43–45] To penetrate the SAS, T cells may first need to cross the blood–CSF barrier in choroid plexus vessels[46] or pial vessels.[47,48] Epifluorescence IVM analysis in the spinal cord vasculature has shown that α_4 integrin controls T-cell

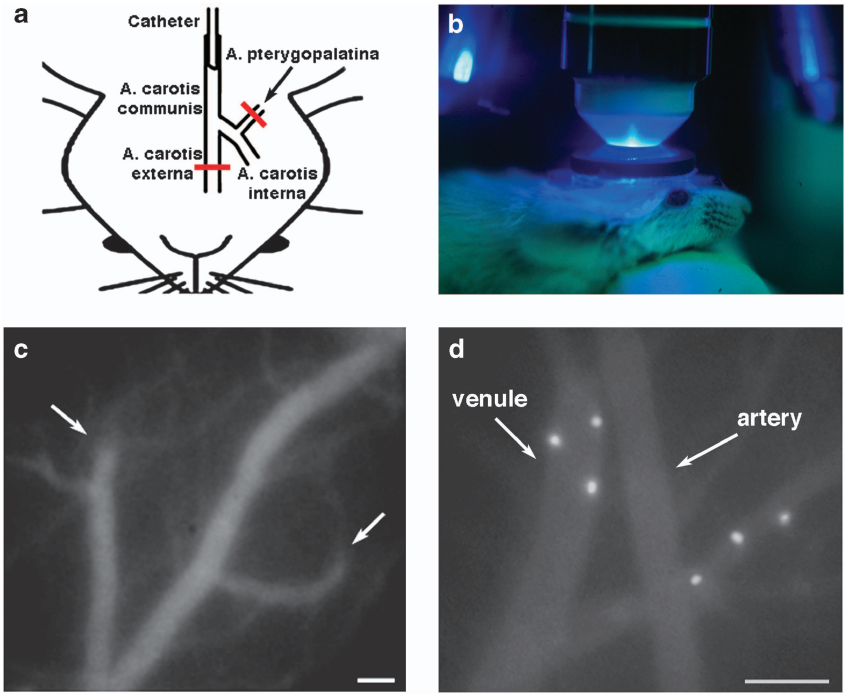

Figure 1 Surgery and epifluorescence IVM imaging of brain pial vessels. (**a**) A heparinized catheter is inserted into the right common carotid artery of anesthetized mice toward the brain. In order to exclude non-cerebral vessels from the analysis, the right external carotid artery and the pterygopalatine artery, a branch from the internal carotid, are ligated (red lines indicate ligatures). (**b**) The scalp is removed, the adherent connective tissue is gently scraped away from the bone and the skull is bathed in sterile saline before a glass coverslip is applied and fixed with silicon grease. A round chamber (~10 mm internal diameter) is then attached to the coverslip with silicon grease and then filled with water to allow the immersion of the microscope objective. A water immersion objective with long focal distance is used to visualize brain vessels through the skull. (**c**) Representative image of brain vessels, labeled by the systemic injection of fluorescent dextran. Pial cortical venules emerge from the deep brain parenchyma to the brain surface, presenting an easily recognizable convex origin (arrow). Scale bar = 100 μm. (**d**) Fluorescence-labeled T_H1 cells injected into LPS-treated mice. Cells are revealed as bright intravascular dots, adhering to the inflamed brain endothelium. Note the lack of adhered cells in the artery. Scale bar = 100 μm.

capture from the bloodstream, whereas integrin LFA-1 is involved in firm adhesion and leukocyte extravasation.[49,50]

Previous IVM studies in spinal cord pial vessels have used a vertebral window over C1–C7, which are not severely affected by EAE.[51] We have recently developed a method allowing the visualization of pial vessels in the lumbar column over L1–L5, which are preferentially targeted by inflammation mechanisms during EAE. Mice are deeply anesthetized using intraperitoneal ketamine/xylazine and then immobilized on a stage under a dissection microscope. After removing the skin, a midline dorsal incision is used to expose the lumbar column over L1–L5. Muscles are dissected from vertebral bones on both sides and a laminectomy is carried out by gentle bone scraping to expose the spinal cord (Figure 2a). This maintains an intact dura mater layer to protect the spinal cord. After surgery, the spinal cord is protected from dehydration and environmental oxygen by adding drops of artificial CSF and sealing with a glass coverslip. A round chamber is attached to the coverslip and filled with water as described above, to allow the immersion of the microscope objective (Figure 2b).

The anatomy of the spinal cord white matter microvasculature is characterized by a large dorsal median vein, which receives veins from the dorsal white matter columns and drains blood caudally. The capillary network is characterized by multiple vessel loops as shown in Figure 2c. Although the blood flow in the major collecting venule shows respiratory-dependent flow motion, blood in the capillary network and post-capillary venules is characterized by physiological hemodynamic parameters.[49]

VIDEO ACQUISITION AND ANALYSIS OF LEUKOCYTE INTERACTIONS

Video images are digitalized and stored using a recorder/converter, allowing data analysis using QuickTime Player or ImageJ software. Vessel diameters (D), hemodynamic parameters and rolling velocities are can be determined using computer-assisted image analysis systems such as NIH Image software. The velocities of 20 consecutive freely flowing cells per venule are determined, allowing the calculation of the velocity of the fastest cell in each venule (V_{max}) and the mean blood flow velocity (V_{mean}) using the formula $V_{mean} = V_{max}/(2-\varepsilon^2)$ where ε is the ratio of cell diameter to vessel diameter. The wall shear rate (WSR), which provides an indication of the force on the vessel wall caused by blood flow, is calculated as follows: $WSR = 8 \times V_{mean}/D$ (s^{-1}). The WSS acting on rolling cells can then be estimated as follows: $WSS = WSR \times 0.025$ (dyne cm^{-2}) assuming a blood viscosity of 0.025 Poise.[52] WSR can influence leukocyte–endothelium interactions under inflammatory conditions, so the above calculations help to ensure that the impact of environmental fluctuations is not included in the final result.[53]

Leukocyte–endothelial cell interactions are usually sampled in venules ranging from 20–100 μm in diameter. Leukocytes are considered to be rolling if they travel at velocities below V_{crit} which is determined as follows: $V_{crit} = V_{mean} \times \varepsilon \times (2-\varepsilon)$.[22,25] Typically, leukocytes are considered to be in adhesion if they are in firm arrest for at least 10–30 s. Cells either rolling or in firm arrest are determined as the percentage of cells that rolled or firmly arrested within a given venule based on the total number of cells that entered

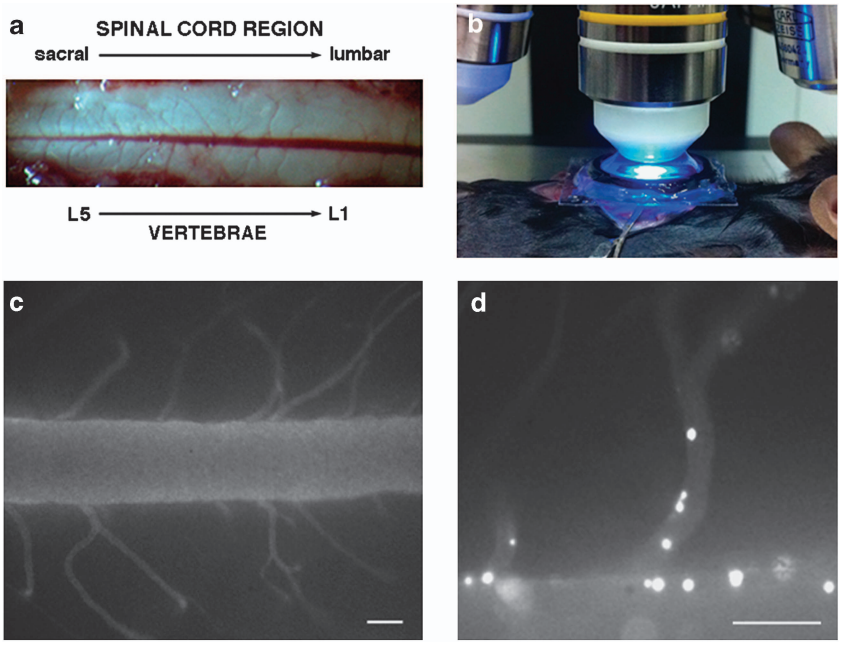

Figure 2 Surgery and epifluorescence IVM imaging of spinal cord venules. A heparinized catheter was inserted into the tail vein of anesthetized mice, to inject fluorescent leukocytes. After skin removal, muscles were dissected from the sides of the vertebral bone and a midline dorsal incision exposed the lumbar column over vertebrae L1–L5. Laminectomy was performed to expose the spinal cord. (**a**) Stereomicroscopic view of exposed spinal cord vessels. (**b**) Exposed spinal cord covered with artificial CSF following surgery. A coverslip is applied on the exposed area. A water immersion objective is used to visualize spinal cord vessels through the intact dura. (**c**) IVM images of exposed spinal cord microcirculation, showing small-diameter pial vessels draining blood flow into the central large collecting venule (dorsal median vein). Spinal cord vessels were visualized by the injection of fluorescent dextran (scale bar = 100 μm). (**d**) Fluorescence-labeled T_H1 cells injected at the disease peak in MOG_{35-55}-immunized EAE mice. Labeled cells can be injected into the tail vein or through a catheter inserted into the carotid artery towards the aortic arch. Cells are revealed as bright intravascular dots, adhering to the inflamed spinal cord endothelium. Note that cells interact with inflamed vessels both in the small-diameter pial venules and in the central large collecting venule (scale bar = 100 μm).

that venule during the same period. Frequency distributions of rolling velocities can also be calculated among the entire leukocyte population. Each of these parameters reflects the action of several distinct molecular pathways with unique biophysical characteristics. Indeed, the adhesion pathways mediating each step of the cascade can vary substantially between different pathological processes, depending on the type and kinetics of the pro-inflammatory stimulus and the nature of the interacting leukocyte subset.

INTRAVITAL TPLSM OF LEUKOCYTE TRAFFICKING IN THE CNS

The recent advent of multiphoton microscopy and transgenic animals that express fluorescent proteins driven by tissue-specific promoters has allowed the direct observation of cell behavior under both physiological and pathological conditions *in vivo*. Pioneering studies have shown that myelin-specific T cells injected in an adoptive transfer model of rat EAE crawl inside spinal cord vessels, subsequently migrating through the endothelium and displaying motility behavior, suggesting that cells resident in the CNS present antigens and activate T cells inside spinal cord parenchyma.[32,54,55] TPLSM studies in a model of viral meningitis have also shown that myelomonocytic cells are massively recruited into the meninges during infection, leading to the loss of BBB integrity and severe seizures.[14] However, there have been few TPLSM studies of the CNS during inflammatory conditions and the motility behavior of leukocyte subpopulations inside CNS vessels, the transmigration mechanisms and the motility behavior inside the parenchyma *in vivo* remain largely unknown.

The interaction between leukocytes and astrocytes, microglia, oligodendrocytes and neurons is also largely uncharacterized *in vivo*. L-selectin has been shown to mediate interactions between lymphocytes and myelin sheets *in vitro*,[56] and adhesion molecules that bind leukocyte counter-receptors are upregulated on neural cells under inflammatory conditions, suggesting potential adhesive interactions between immune cells and neural cells.[57] Furthermore, astrocytes and microglial cells can present antigens to T cells *in vitro*[58] and recent studies have shown that Th17 cells can directly damage neurons *in vitro* by releasing granzyme B.[37] However, the relevance of these neuro-immuno interactions *in vivo* needs to be confirmed by TPLSM imaging.

INTRAVITAL TPLSM IMAGING IN THE CORTEX

Two different surgical preparations can be used for high-resolution *in vivo* imaging: open cranial windows and thinned skull preparations. We and others have found that a thinned skull does not interfere with the visualization of cells up to a depth of 200 μm below the pial surface.[59] This method provides a high-resolution image of the brain tissue while maintaining normal intracerebral pressure and thus preventing mechanical injury and exposure (Figures 3a–c).[14,60] Where higher resolution is required, the brain cortex can be prepared for direct access by opening a 1–2 mm cranial window on the thinned skull area using a needle or forceps. Artificial CSF is applied onto the exposed cortical region. In this case, only cells lying deeper than 80 μm below the pial surface should be considered for image analysis to eliminate possible artifacts caused by surgical preparation.

Long-term imaging can be achieved using mice that are deeply anesthetized, with the head fixed on a stereotaxic device (Figure 3b). Heating is critical for the long-term maintenance of mice under anesthesia, so the core body temperature is monitored and maintained using a regulated heating pad. An incision is made along the midline of the scalp to expose the skull overlying the cortical region of interest. Any fascia overlying the skull is scraped away with a scalpel blade. For thinned skull preparations, a 1–2 mm region on the parietal zone of the skull is thinned using a high-speed micro drill and a stainless steel burr. Drilling is interrupted every few seconds to prevent heating, and bone dust is removed using a can of compressed air. Care should be taken to avoid causing the indentation of the skull during drilling. When the fine vasculature of the dura becomes visible, thinning is continued manually using a microsurgical blade. This process is repeated until the maximum image clarity is achieved (Figure 3a). When imaging is completed, the wound margins of the scalp are closed using a nylon suture.

For the open cranial windows procedure, a circular groove is drilled on the parietal region of the skull and the island of cranial bone is gently removed. The uncovered brain tissue is preserved using a drop of 0.9% NaCl, and when the superficial blood vessels become clearly visible a circular glass coverslip is used to cover the window and part of the skull, and is fixed in place with glue. Following surgical preparation but before image acquisition, mice are given a bolus of warm saline for rehydration and are allowed to recover from anesthesia.

Both skull preparation methods have advantages and disadvantages depending on the purpose of the investigation. The open cranial window method provides excellent optical access to the cortical layers, allowing repeated high-resolution imaging with unlimited time points and arbitrary imaging intervals.[61] This technique is preferable for studies focusing on small structures such as dendritic spines and filopodia.[62] However, removing the skull may induce a significant inflammatory response, involving the activation of microglia and astrocytes in the intact brain.[61,63] Conversely, imaging through the thinned cranial window is a minimally invasive method, which avoids exposing the meninges and the cortex and is therefore more useful for the investigation of normal and pathological processes in the living brain.[61] The thinned cranial preparation allows longer recording periods than an open cranial window because the thinned part of the skull protects the brain from external variations in temperature and pressure. The thinned cranial preparation is preferable for the analysis of structures larger than synaptic connections, such as the movement of leukocytes. Indeed, when following the movement of leukocytes it is important to achieve a wide observation field that allows image-acquisition periods of up to several hours. The thinned cranial preparation also allows imaging immediately after surgery.[61]

INTRAVITAL TPLSM IN THE SPINAL CORD

Most TPLSM studies related to spinal cord pathologies have been carried out on acute slice preparations, but the relevance of these results *in vivo* remains unclear. Only limited imaging work has been carried out on spinal cords in living animals. The close proximity of the heart and lungs to the spinal cord causes artifacts generated by heartbeat and breathing movements, which significantly hinders the acquisition of steady images. Here, we describe a modified method by Davalos *et al.*[64] adapted for lumbar spinal cord, the main site of inflammation in mice with EAE. This new method was recently established in our laboratory and allows the stable imaging of spinal cords in mice with EAE and other spinal cord pathologies.

This method improves firmness by combining a customized spinal stabilization device with deep anesthesia to minimize respiratory movements and allow *in vivo* imaging without intubation or respiratory control. The mice are anesthetized with intraperitoneal ketamine/xylazine before surgery, and afterwards the spinal column is stabilized by mounting Narishige STS-A Compact Spinal Cord Clamps and a Narishige MA-6N head-holding adaptor on a steel

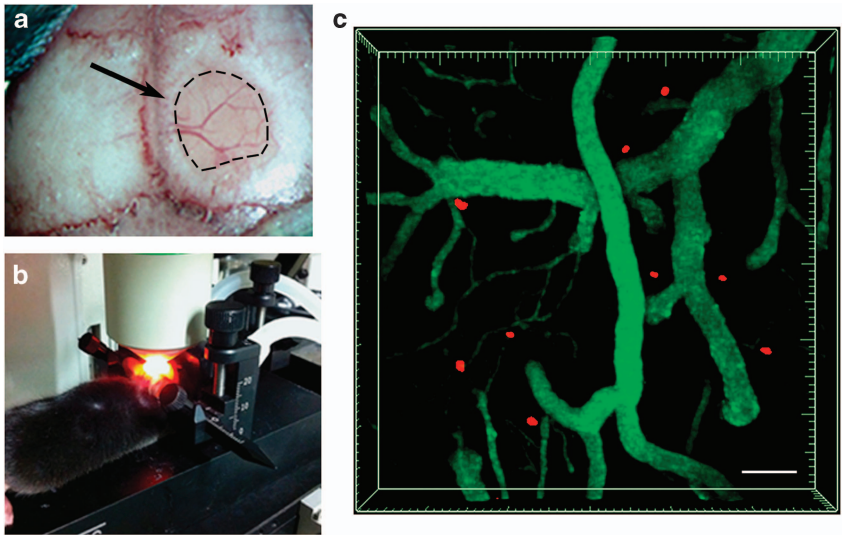

Figure 3 Thinned skull preparation and TPLSM imaging of the brain cortex. (**a**) The hair on the scalp is removed with an electric razor and the scalp is sterilized with alcohol. The head of a deeply anesthetized mouse is fixed on a stereotaxic device, and the skull overlying the cortical region is exposed. A 1–2 mm region on the parietal zone of the skull is thinned using a high-speed micro drill and a stainless steel burr, until the fine vasculature of the dura is visible. The arrow indicates the thinned area enclosed in dashed line. (**b**) Mice are placed under the 20× water immersion objective of a Leica TC5 SP5 confocal-multiphoton microscope. (**c**) Representative two-photon microscopy image of T_H1 cells (red fluorescent spots) injected into C57Bl/6 mice 6 h after the induction of epilepsy with pilocarpine, with the acquisition 16 h after the administration of fluorescent lymphocytes. Cells were labeled with fluorescent tracker CMTPX before injection, while brain cortical vessels (green fluorescence) were labeled by the injection of 525 nm non-targeted quantum dots. Note the presence of T_H1 cells migrated inside the brain parenchyma (scale bar = 30 μm).

base adapted to fit the microscope stage (Figure 4a). After exposing the L1–L5 lumbar column by laminectomy, the muscles are dissected from both sides of the vertebral bone and the paravertebral muscles are retracted to allow the fine tips of the clamping device to be inserted. Artificial CSF is added to allow the direct immersion of the microscope objective (Figure 4a).

Leukocytes can be labeled with vital fluorescent dyes such as CellTracker CMAC (7-amino-4-chloromethylcoumarin), CFSE [5- (and 6-) carboxyfluorescein diacetate succininyl ester] or CMTPX, or they may express fluorescent proteins. After labeling, the leukocytes are resuspended in a small volume of saline and intravenously injected into the tail vein before imaging. To image blood vessels in the cortex or spinal cord, high-molecular-weight fluorescent dextran (>2000 kDa) or non-targeted quantum dots are injected intravenously or retro-orbitally (Figures 3c and 4b).

IMAGE ACQUISITION AND ANALYSIS

During image acquisition, the mice are deeply anesthetized with isofluorane and the rate of respiration is controlled. The laser intensity and PMT gain are set carefully to minimize photodamage, allowing the observation of brain tissue for 4–5 h without affecting normal physiology. The acquisition settings must be chosen carefully based on the behavior of the target cells to ensure successful image analysis. The minimum distance between *z*-planes in the 3D stack should be set on the basis of the axial resolution of the microscope (typically 1–1.5 μm) and on the thickness of the target cells (~4–10 μm for leukocytes).[65] The acquisition rate of current laser scanning microscopes limits the volume of tissue that can be monitored in a given amount of time and hence the duration over which a highly motile cell can be imaged, due to the tendency of the cell to migrate beyond the visual field.[66] This technical limitation could potentially prevent the detection of long-range movement over a chemotactic gradient, which may require imaging over a significant distance and duration.

Fluorescence signals generated by the excitation of multiphoton dyes are acquired in a focal plane section 1–1.5 μm in depth.[67] The objective moves with incremental vertical motion relative to the specimen to yield stacks of optical sections, which are serially reacquired at defined time intervals. In order to track cell motion, it is necessary to determine cell centroids, allowing the migration paths of the cell population to be recorded. Tracks consisting of serial sets of xyz coordinates of single cell centroids are exported as numerical databases and are then used to compute parameters that define cell migration.[66]

Software packages such as Imaris and Volocity are then used for automated 3D cell tracking, so that the acquired tracks can be computed to allow the detailed analysis of individual migration paths. Current algorithms cannot be used to track individual cells under all conditions with 100% reliability, so the results must be examined carefully and manually curated if necessary. Once the cell tracks have been created, several parameters can be used to describe the migration behavior of cells quantitatively. Cell velocity can be analyzed either as instantaneous velocity or track velocity, the former providing a basic parameter derived from the displacement of the cell centroid between adjacent time periods[68] whereas the latter is obtained from the median or mean instantaneous velocity computed from all time intervals throughout a track, typically 6–14 time points at intervals of 20–50 s.[69] The migration properties of cells can also be calculated, for example, if they move along a gradient of soluble or surface-immobilized chemoattractants released from a distant source, providing a chemotactic cue for directed migration. The displacement of an object moving with a constant velocity from an initial position but randomly changing direction is on average linearly proportional to the square root of the elapsed time.[70] The most accurate current method to detect migration patterns is the mean

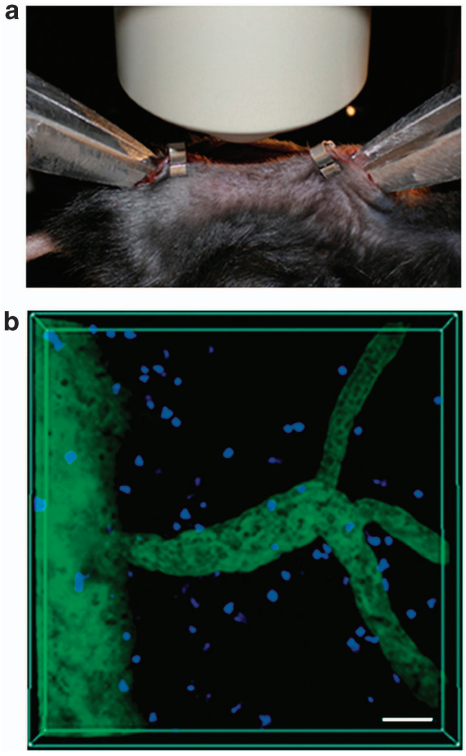

Figure 4 TPLSM imaging of the exposed spinal cord. The surgical procedure used for epifluorescence IVM imaging was carried out for TPLSM imaging (see also Figure 2a). Then, the mouse is positioned on a custom-built stabilizing device to minimize respiratory movements. (**a**) After surgery, the exposed spinal cord is covered with artificial CSF and the surrounding skin meet is tensed and tightened to avoid CSF draining from the tissue. The mouse is placed under the 20× immersion objective of a Leica TC5 SP5 confocal-multiphoton microscope. (**b**) Representative two-photon microscopy image of T_H17 cells (blue fluorescent spots) injected into C57Bl/6 EAE mice, with acquisition 48 h after cell transfer. Cells were labeled with the fluorescent tracker CMFDA before injection, while spinal cord vessels (green fluorescence) were labeled by the systemic injection of 525 nm non-targeted quantum dots (scale bar = 50 μm).

displacement (MD) plot,[68] in which the average displacement of a population of cells over specific time intervals is plotted against the square root of time. The slope of the resulting curve can be used to determine the motility coefficient of a cell population and measures the volume an average cell scans per unit time. If the migration of a cell population follows a random walk model, the curve remains linear during the time interval over which the average cell can be tracked. A plateau after an initial linear segment indicates the confinement of a cell population, for example, by a physical barrier or a biochemical retention signal.[66]

The arrest coefficient is another useful parameter, representing the proportion of time during tracking in which a cell does not move (threshold $<2\,\mu m$ per min). This is the ratio of the time a cell is immobile over the whole observation time. The arrest coefficient is calculated from cell tracks, so the reported value represents a percentage of cells in the entire population.[65] For example, the arrest coefficient is generally high when T cells are in stable contact with other cells or swarm in a chemoattracting microenvironment.[71] A meandering index can also be calculated, based on the ratio of displacement from origin by track length, to provide another index of the directness of cell movement. A meandering index of 0.7–1 generally indicates that cell migration has a strong directional bias, but the more a track deviates from the straight line path, the lower the index, so cells exhibiting frequent angle changes will produce tracks with low meandering indices.[65]

The starting and finishing positions of the tracks can also be used to calculate trajectory vectors representing the direction of displacement of individual cells. The vector–vessel angles of individual tracks can then be determined by mirroring the trajectory vectors onto the nearest vessel (reference vector), resulting in angles of 0–90° for each cell track. This measure is independent of polarized directionality and absolute displacement, making it useful to describe tangential movement along an axis.[72] All these parameters taken together provide vital data on the motility behavior of individual cells, which is particularly important because leukocyte migration depends on the composition and architecture of matrix–protein interactions as determined by the biophysical properties of the extracellular matrix, thus controlling how mechanical forces are transmitted to migrating cells. The matrix composition controls cell adhesion and migration, and its sensitivity to proteolytic enzymes determines the ability of cells to remodel the matrix and migrate through it. The correct evaluation of cell motility behavior therefore requires an experimental setting that can take into account all the microenvironmental complexities known to influence the behavior of migrating leukocytes during immune responses in the CNS.

TPLSM experiments performed by Kawakami *et al.*[54] have analyzed for the first time the dynamic nature of effector T-cell invasion of the CNS. These studies investigated the behavior of encephalitogenic T cells during the early clinical phase of EAE using acute spinal cord slices. The findings showed that effector T cells moved inside the CNS with two distinct migratory patterns: 65% of the T cells moved randomly with high speed through the compact white and gray matter, while 35% of the cells was stationary, suggesting the formation of immune synapses. The analysis of the migratory trajectories showed that the vector sum of their directions and lengths was close to zero confirming a random motility behavior of migrating T cells, whereas stationary T cells seemed to be trapped in their location. Mean square displacement plots also confirmed the morphological observations: they could distinguish two populations, a population with constant displacement over time suggesting freely moving motile T cells and a population of cells that reached a low plateau. The visualization of instantaneous velocity over time shown that this locomotion was not constant, but proceeded in a 'stop and go' mode. As shown for the encephalitogenic T cells, the migratory tracks of non-antigen specific (OVA) T cells within CNS lesions were also random. However, OVA T cells significantly differed from autoreactive T cells by their high proportion of motile cells (95%), as reflected in their higher average velocity and the mean square displacement plots. Treatment of the analyzed tissue with neutralizing anti-MHC class II monoclonal antibodies significantly reduced the number of arrested encephalitogenic T cells, suggesting that T-cell motility within the CNS is dependent on the presence of antigen and MHC class II.[54] These pioneers studies were recently confirmed by TPLSM experiments performed by a laminectomy at the level of the lumbar spinal cord enabling the recording of fluorescent T cells within the meningeal areas and the adjacent white matter.[32,55] In addition, intravital TPLSM studies described the crawling movement of myelin-specific T cells inside the blood vessel, showing that intraluminal T cells moved preferentially against the blood flow.[32] Overall, the motility behavior of encephalitogenic T cells inside the CNS is reminiscent of T cells that migrate through peripheral lymphoid organs with comparable velocities, and along random migration tracks.[73,74]

In the course of autoimmune CNS inflammation, inflammatory infiltrates form characteristic perivascular lymphocyte cuffs by mechanisms that are not well elucidated. Recent intravital TPLSM experiments in mice with EAE have shown the highly dynamic nature of perivascular immune cells in the CNS. These studies elucidated that the motility of extravasated lymphocytes along CNS vessels is an actively CXCR4-dependent mechanism. The analysis of the trajectory vectors and the calculation of the smallest angle between vectors and the nearest vessel axis, allowed Siffrin *et al.*[72] to investigate tangential movement along an axis. Through the comparison of the mean vector–vessel angles, these authors were able to demonstrate that CD4 T cells display a vessel-associated movement, in contrast to CD8 T cells showing a random motility, suggesting a dominant role of the perivascular area primarily for CD4 T cells during autoimmune disease. Moreover, pretreatment with a CXCR4 antagonist led to a shift of CD4 T cells motility from a perivascular motility pattern to intraparenchymal invasion, resulting in disorganization of the vessel cuffs. These data suggest that the compartmentalization of CD4 T-cell motility in vessel proximity is actively promoted, potentially facilitating an efficient and rapid screening of perivascular professional antigen-presenting cells.[72]

Further insight into T-cell motility behavior during EAE came from the analyses of recent intravital TPLSM experiments performed by Kim *et al.*[33] These analyses unveiled that effector T cells migrate preferentially along the rostrocaudal spinal cord axis in the thoracic area during EAE. In order to quantify this biased T-cell motility pattern, the authors aligned the rostrocaudal axis of the spinal cord with the *y*-axis of an analysis grid and plotted the *x* and *y* coordinates of the trajectories obtained from 30 min long intravital movies. They found significantly higher values of displacement in *y* when compared with *x* direction, suggesting that movement was biased along the rostrocaudal axis. Moreover, plotting the displacement in *y* against the square root of time yielded a linear plot suggesting a random walk of T cells along rostrocaudal axis, whereas plotting the *x*-displacement against the square root of time showed a plateau, consistent with constrained motility. This analysis strongly indicated that the cell movement is defined by a rostrocaudal biased random walk with confined lateral movement. However, the mechanisms of this type of movement remain to be elucidated.

FUTURE PERSPECTIVES

Distinct leukocyte populations migrate at selective CNS sites under physiological conditions and during inflammation according to local patterns of endothelial adhesion molecules, chemoattractants, cytokines and danger signals released by neural cells. The molecular mechanisms controlling leukocyte recruitment in the inflamed brain microcirculation have been characterized most thoroughly for Th1 cells and neutrophils, whereas there are little data regarding the mechanisms of other leukocyte subpopulations such as Th17, γδ, iNKT and regulatory cells. In the future, IVM imaging will help to determine how distinct leukocyte populations differentially migrate into the CNS at selected sites, during different neurological pathologies and in relation to the disease phase.

Epifluorescence IVM will help to define the molecular mechanisms controlling the first steps of the adhesion cascade in inflamed CNS venules. Particularly, the investigation of signal transduction pathways controlling leukocyte arrest in CNS venules, which can be explored using selective inhibitors, may provide important information for novel pharmacological interventions. Epifluorescence IVM has been used most frequently to study MS, stroke and infection models, but recent data have shown an unexpected role for leukocyte trafficking in other neurological diseases such as epilepsy. Notably, a recent case report described the efficacy of anti-α4 integrin treatment in refractory epilepsy, confirming the importance of IVM studies for the discovery of novel therapeutic targets for human CNS diseases.[75]

There have been few intravital TPLSM studies in the CNS aiming to define leukocyte trafficking mechanisms. Indeed, the motility behavior of leukocyte subpopulations inside CNS vessels, the transmigration mechanisms and the motility behavior inside the parenchyma remain largely unknown. Transgenic mice expressing fluorescent proteins associated with specific neuronal populations such as neurons,[76] astrocytes,[77] microglia[78] and oligodendrocytes,[79] have become important tools for high-resolution *in vivo* imaging that may help in the future to unravel the mechanisms controlling cell–cell contacts between leukocytes and neural cells. Furthermore, TPLSM may help us to understand how neuronal cells regulate leukocyte infiltration and motility inside the parenchyma, and the functional responses in the CNS by measuring intracellular signaling (for example, the release of Ca^{2+} from neural cells or leukocytes, which cannot be determined by analyzing tissue sections). The study of leukocyte trafficking mechanisms in the CNS and the functional nature of the interactions between neural and immune cells will require interdisciplinary efforts involving immunologists and neuroscientists.

Although TPLSM has proven to be one of the most powerful tools for *in vivo* microscopy, its application to the CNS has been limited to imaging several hundred micrometers below the surface of the cortex. The deeper regions of the brain, such as the hippocampus and striatum for Alzheimer's disease and Parkinson's disease, respectively, are difficult to visualize without excising tissue or performing extensive and complex surgery. The use of gradient index (GRIN) lenses with needle-like dimensions can transfer high-quality images several centimeters from the object plane and could be used visualize deeper brain regions,.[80] Despite the disadvantage of some tissue destruction along the penetration path, this deep imaging technique could be exploited in the future to study the role of leukocyte trafficking in animal models of neurodegenerative diseases. Overall, IVM in animal models of neurological diseases will generate fundamental knowledge to provide insight into the role of the immune system in neurological diseases, and will facilitate the development of novel therapeutic targets for inflammatory CNS diseases.

CONFLICT OF INTEREST

The authors declare no conflict of interest.

ACKNOWLEDGEMENTS

This work was supported in part by the European Research Council Grant 261079 NEUROTRAFFICKING; National Multiple Sclerosis Society (NMSS), New York, NY, USA; Fondazione Cariverona; Italian Ministry of Education and Research (MIUR) and by Fondazione Italiana Sclerosi Multipla (FISM) (to GC).

1 Bechmann I, Galea I, Perry VH. What is the blood-brain barrier (not)? *Trends Immunol* 2007; **28**: 5–11.
2 Ballabh P, Braun A, Nedergaard M. The blood-brain barrier: an overview: structure, regulation, and clinical implications. *Neurobiol Dis* 2004; **16**: 1–13.
3 Rossi B, Angiari S, Zenaro E, Budui SL, Constantin G. Vascular inflammation in central nervous system diseases: adhesion receptors controlling leukocyte-endothelial interactions. *J Leukoc Biol* 2011; **89**: 539–556.
4 Allt G, Lawrenson JG. Is the pial microvessel a good model for blood-brain barrier studies? *Brain Res Brain Res Rev* 1997; **24**: 67–76.

5 Ransohoff RM, Kivisakk P, Kidd G. Three or more routes for leukocyte migration into the central nervous system. *Nat Rev Immunol* 2003; **3**: 569–581.
6 Fletcher JM, Lalor SJ, Sweeney CM, Tubridy N, Mills KH. T cells in multiple sclerosis and experimental autoimmune encephalomyelitis. *Clin Exp Immunol* 2010; **162**: 1–11.
7 Goverman J. Autoimmune T cell responses in the central nervous system. *Nat Rev Immunol* 2009; **9**: 393–407.
8 Price CJ, Warburton EA, Menon DK. Human cellular inflammation in the pathology of acute cerebral ischaemia. *J Neurol Neurosurg Psychiatry* 2003; **74**: 1476–1484.
9 Jin R, Yang G, Li G. Inflammatory mechanisms in ischemic stroke: role of inflammatory cells. *J Leukoc Biol* 2010; **87**: 779–789.
10 Li J, Chang WL, Sun G, Chen HL, Specian RD, Berney SM *et al.* Intercellular adhesion molecule 1 is important for the development of severe experimental malaria but is not required for leukocyte adhesion in the brain. *J Investig Med* 2003; **51**: 128–140.
11 Sun G, Chang WL, Li J, Berney SM, Kimpel D, van der Heyde HC. Inhibition of platelet adherence to brain microvasculature protects against severe Plasmodium berghei malaria. *Infect Immun* 2003; **71**: 6553–6561.
12 Nie CQ, Bernard NJ, Norman MU, Amante FH, Lundie RJ, Crabb BS *et al.* IP-10-mediated T cell homing promotes cerebral inflammation over splenic immunity to malaria infection. *PLoS Pathog* 2009; **5**: e1000369.
13 Fabene PF, Navarro Mora G, Martinello M, Rossi B, Merigo F, Ottoboni L *et al.* A role for leukocyte-endothelial adhesion mechanisms in epilepsy. *Nat Med* 2008; **14**: 1377–1383.
14 Kim JV, Kang SS, Dustin ML, McGavern DB. Myelomonocytic cell recruitment causes fatal CNS vascular injury during acute viral meningitis. *Nature* 2009; **457**: 191–195.
15 Monahan AJ, Warren M, Carvey PM. Neuroinflammation and peripheral immune infiltration in Parkinson's disease: an autoimmune hypothesis. *Cell Transplant* 2008; **17**: 363–372.
16 Kurkowska-Jastrzebska I, Wronska A, Kohutnicka M, Czlonkowski A, Czlonkowska A. MHC class II positive microglia and lymphocytic infiltration are present in the substantia nigra and striatum in mouse model of Parkinson's disease. *Acta Neurobiol Exp* 1999; **59**: 1–8.
17 Butcher EC. Leukocyte-endothelial cell recognition: three (or more) steps to specificity and diversity. *Cell* 1991; **67**: 1033–1036.
18 Springer TA. Traffic signals for lymphocyte recirculation and leukocyte emigration: the multistep paradigm. *Cell* 1994; **76**: 301–314.
19 Ley K, Laudanna C, Cybulsky MI, Nourshargh S. Getting to the site of inflammation: the leukocyte adhesion cascade updated. *Nat Rev Immunol* 2007; **7**: 678–689.
20 Carvalho-Tavares J, Hickey MJ, Hutchison J, Michaud J, Sutcliffe IT, Kubes P. A role for platelets and endothelial selectins in tumor necrosis factor-alpha-induced leukocyte recruitment in the brain microvasculature. *Circ Res* 2000; **87**: 1141–1148.
21 Bertsch T, Kuehl S, Muehlhauser F, Walter S, Hodapp B, Rossol S *et al.* Source of endothelin-1 in subarachnoid hemorrhage. *Clin Chem Lab Med* 2001; **39**: 341–345.
22 Piccio L, Rossi B, Scarpini E, Laudanna C, Giagulli C, Issekutz AC *et al.* Molecular mechanisms involved in lymphocyte recruitment in inflamed brain microvessels: critical roles for P-selectin glycoprotein ligand-1 and heterotrimeric G(i)-linked receptors. *J Immunol* 2002; **168**: 1940–1949.
23 Piccio L, Rossi B, Colantonio L, Grenningloh R, Gho A, Ottoboni L *et al.* Efficient recruitment of lymphocytes in inflamed brain venules requires expression of cutaneous lymphocyte antigen and fucosyltransferase-VII. *J Immunol* 2005; **174**: 5805–5813.
24 Kerfoot SM, Kubes P. Overlapping roles of P-selectin and alpha 4 integrin to recruit leukocytes to the central nervous system in experimental autoimmune encephalomyelitis. *J Immunol* 2002; **169**: 1000–1006.
25 Battistini L, Piccio L, Rossi B, Bach S, Galgani S, Gasperini C *et al.* CD8 + T cells from patients with acute multiple sclerosis display selective increase of adhesiveness in brain venules: a critical role for P-selectin glycoprotein ligand-1. *Blood* 2003; **101**: 4775–4782.
26 Kerfoot SM, Norman MU, Lapointe BM, Bonder CS, Zbytnuik L, Kubes P. Reevaluation of P-selectin and alpha 4 integrin as targets for the treatment of experimental autoimmune encephalomyelitis. *J Immunol* 2006; **176**: 6225–6234.
27 Denk W, Delaney KR, Gelperin A, Kleinfeld D, Strowbridge BW, Tank DW *et al.* Anatomical and functional imaging of neurons using 2-photon laser scanning microscopy. *J Neurosci Methods* 1994; **54**: 151–162.
28 Grutzendler J, Kasthuri N, Gan WB. Long-term dendritic spine stability in the adult cortex. *Nature* 2002; **420**: 812–816.
29 Stosiek C, Garaschuk O, Holthoff K, Konnerth A. *In vivo* two-photon calcium imaging of neuronal networks. *Proc Natl Acad Sci USA* 2003; **100**: 7319–7324.
30 Yoder EJ, Kleinfeld D. Cortical imaging through the intact mouse skull using two-photon excitation laser scanning microscopy. *Microsc Res Tech* 2002; **56**: 304–305.
31 Klunk WE, Bacskai BJ, Mathis CA, Kajdasz ST, McLellan ME, Frosch MP *et al.* Imaging Abeta plaques in living transgenic mice with multiphoton microscopy and methoxy-X04, a systemically administered Congo red derivative. *J Neuropathol Exp Neurol* 2002; **61**: 797–805.
32 Bartholomaus I, Kawakami N, Odoardi F, Schlager C, Miljkovic D, Ellwart JW *et al.* Effector T cell interactions with meningeal vascular structures in nascent autoimmune CNS lesions. *Nature* 2009; **462**: 94–98.
33 Kim JV, Jiang N, Tadokoro CE, Liu L, Ransohoff RM, Lafaille JJ *et al.* Two-photon laser scanning microscopy imaging of intact spinal cord and cerebral cortex reveals requirement for CXCR6 and neuroinflammation in immune cell infiltration of cortical injury sites. *J Immunol Methods* 2010; **352**: 89–100.
34 McGavern DB, Kang SS. Illuminating viral infections in the nervous system. *Nat Rev Immunol* 2011; **11**: 318–329.
35 Galea I, Bechmann I, Perry VH. What is immune privilege (not)? *Trends Immunol* 2007; **28**: 12–18.
36 Bolton SJ, Anthony DC, Perry VH. Loss of the tight junction proteins occludin and zonula occludens-1 from cerebral vascular endothelium during neutrophil-induced blood-brain barrier breakdown *in vivo*. *Neuroscience* 1998; **86**: 1245–1257.
37 Kebir H, Kreymborg K, Ifergan I, Dodelet-Devillers A, Cayrol R, Bernard M *et al.* Human TH17 lymphocytes promote blood-brain barrier disruption and central nervous system inflammation. *Nat Med* 2007; **13**: 1173–1175.
38 Hildebrandt M, Amann K, Schroder R, Pieper T, Kolodziejczyk D, Holthausen H *et al.* White matter angiopathy is common in pediatric patients with intractable focal epilepsies. *Epilepsia* 2008; **49**: 804–815.
39 Scremin OU. Cerebral Vascular System. In: Paxinos G (ed.) *The Rat Nervous System*. Second edition, 1995.
40 Ley K, Gaehtgens P. Endothelial, not hemodynamic, differences are responsible for preferential leukocyte rolling in rat mesenteric venules. *Circ Res* 1991; **69**: 1034–1041.
41 Mazo IB, Gutierrez-Ramos JC, Frenette PS, Hynes RO, Wagner DD, von Andrian UH. Hematopoietic progenitor cell rolling in bone marrow microvessels: parallel contributions by endothelial selectins and vascular cell adhesion molecule 1. *J Exp Med* 1998; **188**: 465–474.
42 Rovainen CM, Woolsey TA, Blocher NC, Wang DB, Robinson OF. Blood flow in single surface arterioles and venules on the mouse somatosensory cortex measured with videomicroscopy, fluorescent dextrans, nonoccluding fluorescent beads, and computer-assisted image analysis. *J Cereb Blood Flow Metab* 1993; **13**: 359–371.
43 Lassmann H, Wisniewski HM. Chronic relapsing EAE. Time course of neurological symptoms and pathology. *Acta Neuropathol* 1978; **43**: 35–42.
44 Traugott U, Raine CS. Acute experimental allergic encephalomyelitis. Myelin basic protein-reactive T cells in the circulation and in meningeal infiltrates. *J Neurol Sci* 1979; **42**: 331–336.
45 Tsuchida M, Hanawa H, Hirahara H, Watanabe H, Matsumoto Y, Sekikawa H *et al.* Identification of CD4- CD8- alpha beta T cells in the subarachnoid space of rats with experimental autoimmune encephalomyelitis. A possible route by which effector cells invade the lesions. *Immunology* 1994; **81**: 420–427.
46 Reboldi A, Coisne C, Baumjohann D, Benvenuto F, Bottinelli D, Lira S *et al.* C-C chemokine receptor 6-regulated entry of TH-17 cells into the CNS through the choroid plexus is required for the initiation of EAE. *Nat Immunol* 2009; **10**: 514–523.
47 Kivisakk P, Imitola J, Rasmussen S, Elyaman W, Zhu B, Ransohoff RM *et al.* Localizing central nervous system immune surveillance: meningeal antigen-presenting cells activate T cells during experimental autoimmune encephalomyelitis. *Ann Neurol* 2009; **65**: 457–469.
48 Brown DA, Sawchenko PE. Time course and distribution of inflammatory and neurodegenerative events suggest structural bases for the pathogenesis of experimental autoimmune encephalomyelitis. *J Comp Neurol* 2007; **502**: 236–260.
49 Vajkoczy P, Laschinger M, Engelhardt B. Alpha4-integrin-VCAM-1 binding mediates G protein-independent capture of encephalitogenic T cell blasts to CNS white matter microvessels. *J Clin Invest* 2001; **108**: 557–565.
50 Bauer M, Brakebusch C, Coisne C, Sixt M, Wekerle H, Engelhardt B *et al.* Beta1 integrins differentially control extravasation of inflammatory cell subsets into the CNS during autoimmunity. *Proc Natl Acad Sci USA* 2009; **106**: 1920–1925.
51 Engelhardt B, Vajkoczy P, Laschinger M. Detection of endothelial/lymphocyte interaction in spinal cord microvasculature by intravital videomicroscopy. *Methods Mol Med* 2003; **89**: 83–93.
52 Von Andrian UH, Hansell P, Chambers JD, Berger EM, Torres Filho I, Butcher EC *et al.* L-selectin function is required for beta 2-integrin-mediated neutrophil adhesion at physiological shear rates *in vivo*. *Am J Physiol* 1992; **263**: H1034–H1044.
53 Sumagin R, Lamkin-Kennard KA, Sarelius IH. A separate role for ICAM-1 and fluid shear in regulating leukocyte interactions with straight regions of venular wall and venular convergences. *Microcirculation* 2009; **16**: 508–520.
54 Kawakami N, Nagerl UV, Odoardi F, Bonhoeffer T, Wekerle H, Flugel A. Live imaging of effector cell trafficking and autoantigen recognition within the unfolding autoimmune encephalomyelitis lesion. *J Exp Med* 2005; **201**: 1805–1814.
55 Odoardi F, Kawakami N, Li Z, Cordiglieri C, Streyl K, Nosov M *et al.* Instant effect of soluble antigen on effector T cells in peripheral immune organs during immunotherapy of autoimmune encephalomyelitis. *Proc Natl Acad Sci USA* 2007; **104**: 920–925.
56 Huang K, Geoffroy JS, Singer MS, Rosen SD. A lymphocyte homing receptor (L-selectin) mediates the *in vitro* attachment of lymphocytes to myelinated tracts of the central nervous system. *J Clin Invest* 1991; **88**: 1778–1783.
57 Raine CS. Multiple sclerosis: immune system molecule expression in the central nervous system. *J Neuropathol Exp Neurol* 1994; **53**: 328–337.
58 Hamo L, Stohlman SA, Otto-Duessel M, Bergmann CC. Distinct regulation of MHC molecule expression on astrocytes and microglia during viral encephalomyelitis. *Glia* 2007; **55**: 1169–1177.
59 Nimmerjahn A, Kirchhoff F, Helmchen F. Resting microglial cells are highly dynamic surveillants of brain parenchyma *in vivo*. *Science* 2005; **308**: 1314–1318.
60 Davalos D, Grutzendler J, Yang G, Kim JV, Zuo Y, Jung S *et al.* ATP mediates rapid microglial response to local brain injury *in vivo*. *Nat Neurosci* 2005; **8**: 752–758.
61 Yang G, Pan F, Parkhurst CN, Grutzendler J, Gan WB. Thinned-skull cranial window technique for long-term imaging of the cortex in live mice. *Nat Protoc* 2010; **5**: 201–208.
62 Majewska AK, Newton JR, Sur M. Remodeling of synaptic structure in sensory cortical areas *in vivo*. *J Neurosci* 2006; **26**: 3021–3029.
63 Xu HT, Pan F, Yang G, Gan WB. Choice of cranial window type for *in vivo* imaging affects dendritic spine turnover in the cortex. *Nat Neurosci* 2007; **10**: 549–551.
64 Davalos D, Lee JK, Smith WB, Brinkman B, Ellisman MH, Zheng B *et al.* Stable *in vivo* imaging of densely populated glia, axons and blood vessels in the mouse spinal cord using two-photon microscopy. *J Neurosci Methods* 2008; **169**: 1–7.

65 Zinselmeyer BH, Dempster J, Wokosin DL, Cannon JJ, Pless R, Parker I *et al*. Chapter 16Two-photon microscopy and multidimensional analysis of cell dynamics. *Methods Enzymol* 2009; **461**: 349–378.
66 Sumen C, Mempel TR, Mazo IB, von Andrian UH. Intravital microscopy: visualizing immunity in context. *Immunity* 2004; **21**: 315–329.
67 Denk W, Strickler JH, Webb WW. Two-photon laser scanning fluorescence microscopy. *Science* 1990; **248**: 73–76.
68 Miller MJ, Wei SH, Parker I, Cahalan MD. Two-photon imaging of lymphocyte motility and antigen response in intact lymph node. *Science* 2002; **296**: 1869–1873.
69 Aoshi T, Zinselmeyer BH, Konjufca V, Lynch JN, Zhang X, Koide Y *et al*. Bacterial entry to the splenic white pulp initiates antigen presentation to CD8+ T cells. *Immunity* 2008; **29**: 476–486.
70 Wei SH, Parker I, Miller MJ, Cahalan MD. A stochastic view of lymphocyte motility and trafficking within the lymph node. *Immunol Rev* 2003; **195**: 136–159.
71 Tadokoro CE, Shakhar G, Shen S, Ding Y, Lino AC, Maraver A *et al*. Regulatory T cells inhibit stable contacts between CD4+ T cells and dendritic cells *in vivo*. *J Exp Med* 2006; **203**: 505–511.
72 Siffrin V, Brandt AU, Radbruch H, Herz J, Boldakowa N, Leuenberger T *et al*. Differential immune cell dynamics in the CNS cause CD4+ T cell compartmentalization. *Brain* 2009; **132**: 1247–1258.
73 Miller MJ, Wei SH, Cahalan MD, Parker I. Autonomous T cell trafficking examined *in vivo* with intravital two-photon microscopy. *Proc Natl Acad Sci USA* 2003; **100**: 2604–2609.
74 Bousso P. T-cell activation by dendritic cells in the lymph node: lessons from the movies. *Nat Rev Immunol* 2008; **8**: 675–684.
75 Sotgiu S, Murrighile MR, Constantin G. Treatment of refractory epilepsy with natalizumab in a patient with multiple sclerosis. Case report. *BMC Neurol* 2010; **10**: 84.
76 Feng G, Mellor RH, Bernstein M, Keller-Peck C, Nguyen QT, Wallace M *et al*. Imaging neuronal subsets in transgenic mice expressing multiple spectral variants of GFP. *Neuron* 2000; **28**: 41–51.
77 Petzold GC, Murthy VN. Role of astrocytes in neurovascular coupling. *Neuron* 2011; **71**: 782–797.
78 Vukovic J, Colditz MJ, Blackmore DG, Ruitenberg MJ, Bartlett PF. Microglia modulate hippocampal neural precursor activity in response to exercise and aging. *J Neurosci* 2012; **32**: 6435–6443.
79 Fuss B, Mallon B, Phan T, Ohlemeyer C, Kirchhoff F, Nishiyama A *et al*. Purification and analysis of *in vivo*-differentiated oligodendrocytes expressing the green fluorescent protein. *Dev Biol* 2000; **218**: 259–274.
80 Levene MJ, Dombeck DA, Kasischke KA, Molloy RP, Webb WW. *In vivo* multiphoton microscopy of deep brain tissue. *J Neurophysiol* 2004; **91**: 1908–1912.